Received: 26 August 2021 | Revised: 28 October 2021 | Accepted: 29 October 2021

DOI: 10.1002/jcla.24116

RESEARCH ARTICLE

WILEY

Circ_0000463 contributes to the progression and glutamine metabolism of non-small-cell lung cancer by targeting miR-924/SLC1A5 signaling

Yunzhong Liu[1] | Shujun Wang[1] | Songli Pan[2] | Qingfeng Yan[3] | Yueping Li[4] | Ying Zhao[1]

[1]Department of Cardio and Thoracic Surgery, The First Affiliated Hospital of Hainan Medical University, Haikou, China

[2]Department of Orthopaedic, The First Affiliated Hospital of Hainan Medical University, Haikou, China

[3]Department of Pathophysiology, Hainan Medical College, Haikou, China

[4]Department of Histology and Embryology, Hainan Medical College, Haikou, China

Correspondence
Ying Zhao, Department of Cardio and Thoracic Surgery, The First Affiliated Hospital of Hainan Medical University, 31 Longhua Road, Haikou 570102, Hainan, China.
Email: zylhainan@126.com.

Funding information
This work was supported by the Research Project of health industry in Hainan Province (No. 20A200142)

Abstract

Background: Circular RNAs (circRNAs) have shown pivotal regulatory roles in the pathology of non-small cell lung cancer (NSCLC). However, the role of circ_0000463 in NSCLC progression and its associated molecular mechanism remain to be illustrated.

Methods: Cell proliferation ability was analyzed by colony formation assay and 5-ethynyl-2'-deoxyuridine (EdU) assay. Cell migration and invasion abilities were assessed by scratch test and transwell invasion assay. Flow cytometry was employed to analyze cell apoptotic rate. The interaction between microRNA-924 (miR-924) and circ_0000463 or solute carrier family 1 member 5 (SLC1A5) was confirmed by dual-luciferase reporter assay and RNA immunoprecipitation (RIP) assay. The uptake of glutamine and the production of glutamate and α-ketoglutarate were analyzed using their corresponding kits. Xenograft model in vivo was established to analyze the role of circ_0000463 in tumor growth.

Results: Circ_0000463 expression was elevated in NSCLC tissues and cell lines. Circ_0000463 knockdown suppressed the proliferation, migration, and invasion and promoted the apoptosis of NSCLC cells. Circ_0000463 acted as a molecular sponge for miR-924, and circ_0000463 interference-mediated anti-tumor effects were largely reversed by the silence of miR-924 in NSCLC cells. miR-924 interacted with the 3' untranslated region (3'UTR) of SLC1A5, and SLC1A5 overexpression largely overturned miR-924 overexpression-mediated anti-tumor effects in NSCLC cells. Moreover, circ_0000463 absence suppressed the glutamine metabolism of NSCLC cells by targeting miR-924/SLC1A5 axis. Circ_0000463 knockdown suppressed xenograft tumor growth in vivo.

Conclusion: Circ_0000463 absence suppressed the malignant behaviors and glutamine metabolism of NSCLC cells through mediating miR-924/SLC1A5 axis.

KEYWORDS
circ_0000463, glutamine metabolism, miR-924, non-small-cell lung cancer, SLC1A5

1 | INTRODUCTION

Lung cancer is a common malignancy with high morbidity and mortality.[1] Among which, non-small cell lung cancer (NSCLC) accounts for 85% of all lung cancer cases.[2] Although the progression in the diagnosis of NSCLC and the emergence of a new generation of targeted drugs, patients with NSCLC still have a poor prognosis and a high recurrence rate.[3] Uncovering the pathologic mechanism of NSCLC is essential for the development of effective therapeutic methods.

Circular RNAs (circRNAs) are ideal bio-markers due to their high stability and tissue-specific expression pattern.[4] CircRNAs are implicated in the progression of NSCLC. For instance, circ_0001869 is reported to facilitate the growth and motility of NSCLC cells.[5] Circ_0000376 is reported to promote the growth, metastasis, and chemo-resistance of NSCLC cells.[6] A previous study reported that circ_0000463 expression is upregulated in lung cancer.[7] Nevertheless, the function of circ_0000463 in NSCLC progression and its associated mechanism remain unclear.

Accumulating evidence have demonstrated that circRNAs can act as molecular sponges for microRNAs (miRNAs), thus negatively regulating miRNA expression and further controlling the levels of downstream genes.[8–10] Through bioinformatics analysis, miR-924 was predicted as a potential target of circ_0000463 in this study. Previous articles reported that miR-924 plays an anti-tumor role in hepatocellular carcinoma[11] and NSCLC.[12] For example, Fan et al. demonstrated that lncRNA n335586 contributes to hepatocellular carcinoma development by absorbing miR-924,[11] indicating the anti-tumor role of miR-924 in hepatocellular carcinoma. miR-924 is reported to reduce the malignant potential of NSCLC cells by negatively regulating RHBDD1 expression and inactivating Wnt/β-catenin pathway.[12] Here, we tested the binding relationship between circ_0000463 and miR-924 in NSCLC cells and further explored their functional correlation in NSCLC progression.

Solute carrier family 1 member 5 (SLC1A5) is responsible for the transportation of glutamine.[13] Previous researchers confirmed that SLC1A5 contributes to cancer progression by promoting glutamine metabolism.[14–16] Silencing the expression of SLC1A5 is reported to restrain the survival of lung cancer cells by reducing glutamine transportation.[17] SLC1A5 is also reported to contribute to the growth and motility and suppress the apoptotic rate of NSCLC cells.[18] Bioinformatics software predicted that SLC1A5 was a potential target of miR-924 in this study. The associated relation between miR-924 and SLC1A5 was tested, and their functional correlation was further investigated.

In this study, we first analyzed the expression pattern and biological function of circ_0000463 in NSCLC. Then, the downstream miRNA/mRNA axis of circ_0000463 was predicted by bioinformatics analysis and verified by rescue experiments. This study will provide more insights into the pathogenesis of NSCLC.

2 | MATERIALS AND METHODS

2.1 | Tissue collection

Sixty-five pairs of NSCLC tissues and adjacent healthy tissues were collected from NSCLC patients during surgical resection at the First Affiliated Hospital of Hainan Medical University. The tissue samples were stored at −80℃ before use. The written informed consent had been signed by all the NSCLC patients before the surgery. Clinical study was authorized by the ethics committee of the First Affiliated Hospital of Hainan Medical University and in compliance with the guidelines of the Declaration of Helsinki.

2.2 | Cell culture

Non-small cell lung cancer cell lines (NCI-H1299, HCC827, A549, and H460) and normal human bronchial epithelioid cell line 16HBE were purchased from American Type Culture Collection (Manassas, VA, USA). All the cell lines were cultured with Roswell Park Memorial Institute-1640 medium (RPMI-1640, Gibco) added with 10% fetal bovine serum (FBS, Gibco) and 1% antibiotic mixture (Sangon Biotech) under the standard culture condition (37℃ and 5% CO_2).

2.3 | Verification of circular structure of circ_0000463

For RNase R treatment, RNA samples were incubated with 100 μg/ml RNase R (Applied Biological Materials, Vancouver, Canada) at 37℃ for 30 min. For actinomycin D treatment, NSCLC cells were incubated with 2 mg/ml actinomycin D (Sigma) and collected at the preset time points. RT-qPCR was conducted to measure RNA levels.

2.4 | Reverse transcription-quantitative polymerase chain reaction (RT-qPCR)

TRIzol reagent (Invitrogen) was utilized during RNA isolation. For circ_0000463, EP400NL, and SLC1A5, High Capacity cDNA Kit (Thermo Fisher Scientific) was utilized to obtain complementary DNA (cDNA), which was subsequently utilized as the template for thermal cycling reaction with SYBR Green qPCR Mix (Bio-Rad). Glyceraldehyde 3-phosphate dehydrogenase (GAPDH) was used as the reference for the normalization of circ_0000463, EP400NL, and SLC1A5 expression. For miR-924, miRNA-specific stem-loop reverse transcription primer (Ribobio) was used for reverse transcription, and amplification reaction was conducted using miRNA-specific forward primer and universal primer. U6 was utilized as the reference for the normalization of miR-924 expression. The relative abundance was calculated as $2^{-\Delta\Delta Ct}$. All primers are listed in Table 1.

TABLE 1 Primer sequences in RT-qPCR assay

Gene	Sequence (5′-3′)
circ_0000463	Forward: ACTCAGCATGACCTCCGTTC
	Reverse: AGTCACGGCAGCAGGAGTAG
EP400NL	Forward: ACCAGAGAAATCGAGCGTCC
	Reverse: CACTTGTGTGGTTGGCTGTG
miR−924	Forward: GGCCAGAGTCTTGTGATG
	Reverse: GCAGGGTCCGAGGTATTC
SLC1A5	Forward: CTCCAGCCCTCGGGAGTAAA
	Reverse: CGGATAAGCAGCTCCCCTTC
U6	Forward: GCTTCGGCAGCACATATACTAAAAT
	Reverse: CGCTTCACGAATTTGCGTGTCAT
GAPDH	Forward: TATGATGACATCAAGAAGGTGGT
	Reverse: TGTAGCCAAATTCGTTGTCATAC

2.5 | Cell transfection

Short hairpin (sh)RNA against circ_0000463 (sh-circ_0000463), matched negative control (sh-NC), mimics of miR-924 (miR-924), miR-NC, inhibitor of miR-924 (in-miR-924), in-miR-NC, SLC1A5 plasmid (SLC1A5), and pcDNA were purchased from Genepharma (Shanghai, China). Lipofectamine™ 3000 transfection reagent (Invitrogen) was utilized to introduce small RNAs or plasmids into NSCLC cells during transient transfection.

2.6 | Colony formation assay

Non-small cell lung cancer cells in 12-well plates (200 cells/well) were continued to culture for 14 days under the standard culture condition. The culture medium was replenished every 4 days. The culture supernatant was discarded after 14 days incubation, and colonies were rinsed with phosphate-buffered saline (PBS) solution twice. After staining with 0.5% crystal violet (Sangon Biotech) for 20 min, the number of colonies was analyzed.

2.7 | 5-ethynyl-2'-deoxyuridine (EdU) assay

Non-small cell lung cancer cells were incubated with 50 μM EdU solution (Ribobio) to mark the synthesized DNA, and cell nucleus was stained with 4,6-diamino-2-phenyl indole (DAPI; Sigma). Cell images were captured, and the proportion of EdU^+ cells was analyzed.

2.8 | Scratch test

When cell confluence reached about 95%, cell monolayer was scraped with a pipette tip. Cell debris and unattached cells were discarded by washing with PBS thrice. Micrographs were taken at 0 h and 24 h after creating the gap.

2.9 | Transwell invasion assay

The top side of polycarbonate Transwell filter of the upper chambers was coated with Matrigel (BD Biosciences). NSCLC cells (8×10^4) in serum-free medium were seeded over the Matrigel in upper chambers, with the below chambers added with 10% FBS (chemoattractant)-contained medium. NSCLC cells were cultured for 48 h. Cells on the top side of the transwell filter were scraped out, and invaded cells were dyed with 0.1% crystal violet (Sangon Biotech). The number of invaded cells was counted under a microscope (five random fields of view at 100×).

2.10 | Flow cytometry

Annexin V-fluorescein isothiocyanate (FITC)/propidium iodide (PI) kit (Beyotime) was adopted to analyze cell apoptosis. After transfection for 72 h, NSCLC cells were collected and suspended in 100 μl binding buffer. Then, 10 μl of Annexin V-FITC and 10 μl of PI were simultaneously incubated with NSCLC cells for 15 min at room temperature in the dark. The percentage of apoptotic cells was assessed by flow cytometer.

2.11 | Western blot assay

Non-small cell lung cancernon-small cell lung cancer cells were disrupted with Western cell lysis buffer (Beyotime), and the concentrations of protein samples were determined using the bicinchoninic acid (BCA) kit (Pierce Biotech). After separating by 10% separating gel, the protein samples were transferred onto the polyvinylidene difluoride (PVDF) membrane (Millipore). The membrane was sealed with 5% non-fat milk and labeled with primary antibodies (Abcam) overnight at 4℃, including anti-proliferating cell nuclear antigen (anti-PCNA, ab280088, dilution of 1:1000), anti-E-cadherin (ab238099, dilution of 1:3000), anti-Bcl-2 associated X, apoptosis regulator (anti-Bax, ab32503, dilution of 1:8000), anti-SLC1A5 (ab237704, dilution of 1:1000), and anti-GAPDH (ab8245, dilution of 1:10000). The membrane was then incubated with the secondary antibody (Abcam) for 2 h at room temperature. The protein signals were analyzed using the enhanced chemiluminescence reagents (Pierce Biotech). Image Lab analysis software (Bio-Rad) was used to analyze the intensities of protein bands.

2.12 | Establishment of circRNA/miRNA/messenger RNA (mRNA) signaling axis

Bioinformatics software circinteractome (https://circinteractome.irp.nia.nih.gov) or targetscan (http://www.targetscan.org) was used to predict circ_0000463-miRNA interactions or miR-924-mRNA interactions, respectively.

2.13 | Dual-luciferase reporter assay

The wild-type partial sequence of circ_0000463 or SLC1A5, including the putative binding sites of miR-924, was inserted into commercial luciferase pmirGLO vector (Promega) to generate circ_0000463 WT or SLC1A5 3' untranslated region (3'UTR) WT. Similarly, circ_0000463 MUT or SLC1A5 3'UTR MUT was constructed. For the luciferase activity analysis, NSCLC cells were co-introduced with small RNAs and luciferase reporter plasmids. After transfection for 48 h, the luciferase intensities were analyzed.

2.14 | RNA immunoprecipitation (RIP) assay

A Magna RNA immunoprecipitation kit (Millipore) was adopted for RIP assay to confirm the associated relation between circ_0000463 and miR-924. NSCLC cells were introduced with miR-924 mimics for 48 h and then cells were disrupted using ice-cold radio-Immunoprecipitation Assay (RIPA) lysis buffer. Cell extracts were mixed with anti-Argonaute 2 (Anti-Ago2; Abcam) or anti-Immunoglobulin G (Anti-IgG; Abcam) for 4 h at 4℃. Then, the magnetic protein A/G beads were added to incubate for 2 h. Beads were washed with PBS thrice, and RT-qPCR was applied to measure RNA enrichment.

2.15 | Analysis of glutamine metabolism

The consumption of glutamine and the production of glutamate and α-ketoglutarate were analyzed using glutamine assay kit (Abcam), glutamate assay kit (Abcam), and α-ketoglutarate assay kit (Abcam).

2.16 | Xenograft model in vivo

A total of ten BALB/c male nude mice (4–6 weeks old, 18–22 g) were purchased from Vital River Laboratory Animal Technology (Beijing, China) after obtaining the approval of the Animal Ethical Committee of the First Affiliated Hospital of Hainan Medical University. Animal experiment was conducted in compliance with the ARRIVE guidelines and all nude mice received humane care according to the National Institutes of Health (USA) guidelines. Nude mice were maintained in pathogen-free condition with a 12-h light/dark cycle at 22 ± 1℃ and 60% humidity. These nude mice were supplied food and water *ad libitum*. The weight of mice was measured twice a week to monitor the health of mice. The mice were arbitrarily divided into two groups: (1) sh-NC group: The right flank of mice were subcutaneously injected with A549 cells (2.0×10^5 cells; 200 μl cell suspension) stably expressing sh-NC. 2) sh-circ_0000463 group: The right flank of mice were subcutaneously injected with A549 cells (2.0×10^5 cells; 200 μl cell suspension) stably expressing sh-circ_0000463. Tumor size was detected every 7 d as length × width^2 × 0.5. The maximum of tumor volume was no more than 1000 mm^3. After inoculation for 35 days, the mice were euthanized by carbon dioxide suffocation (30% chamber volume/min), and the xenograft tumors were taken out and weighed using an analytical balance. RT-qPCR, western blot assay, and IHC assay were conducted to analyze the expression of key molecules.

2.17 | Data analysis

The results were processed using GraphPad Prism software and represented as mean ± standard deviation (SD). Statistical significance was analyzed using Student's *t* test for the data in two groups or one-way analysis of variance (ANOVA) followed by Tukey's test for the data in multiple groups. Linear regression analysis was carried out using Pearson's correlation analysis. Values of $p < 0.05$ were designated as statistically significant.

3 | RESULTS

3.1 | Circ_0000463 expression is significantly upregulated in NSCLC tissues and cell lines

Circ_0000463 is a circular transcript derived from the back-splicing of its host gene EP400NL. The chromosomal location of circ_0000463 is shown in Figure 1A. We analyzed the expression pattern of circ_0000463 in NSCLC and found that circ_0000463 was significantly upregulated in NSCLC tissues and cell lines (especially in A549 and H460 cell lines) compared with adjacent normal tissues and 16HBE cell line (Figure 1B, C). Therefore, we chose A549 and H460 cell lines for the following experiments. RNase R treatment assay displayed that circ_0000463 expression remained unchanged in RNase R treatment group and Mock group, while RNase R treatment markedly reduced the level of linear EP400NL (Figure 1D, E), suggesting that circ_0000463 was resistant to RNase R. The stability of circ_0000463 was analyzed using transcriptional inhibitor actinomycin D. Circ_0000463 level was stable upon actinomycin D treatment, whereas the level of EP400NL was notably reduced in a time-dependent manner (Figure 1F, G), demonstrating that circ_0000463 was stably existed in NSCLC cells. These results suggested that circ_0000463 expression might be associated with the progression of NSCLC.

3.2 | Circ_0000463 absence suppresses the malignant behaviors of NSCLC cells

We explored the biological role of circ_0000463 in NSCLC cells by loss-of-function experiments. A549 and H460 cell lines stably expressing sh-NC or sh-circ_0000463 were established. RT-qPCR assay showed that sh-circ_0000463 was effective in silencing

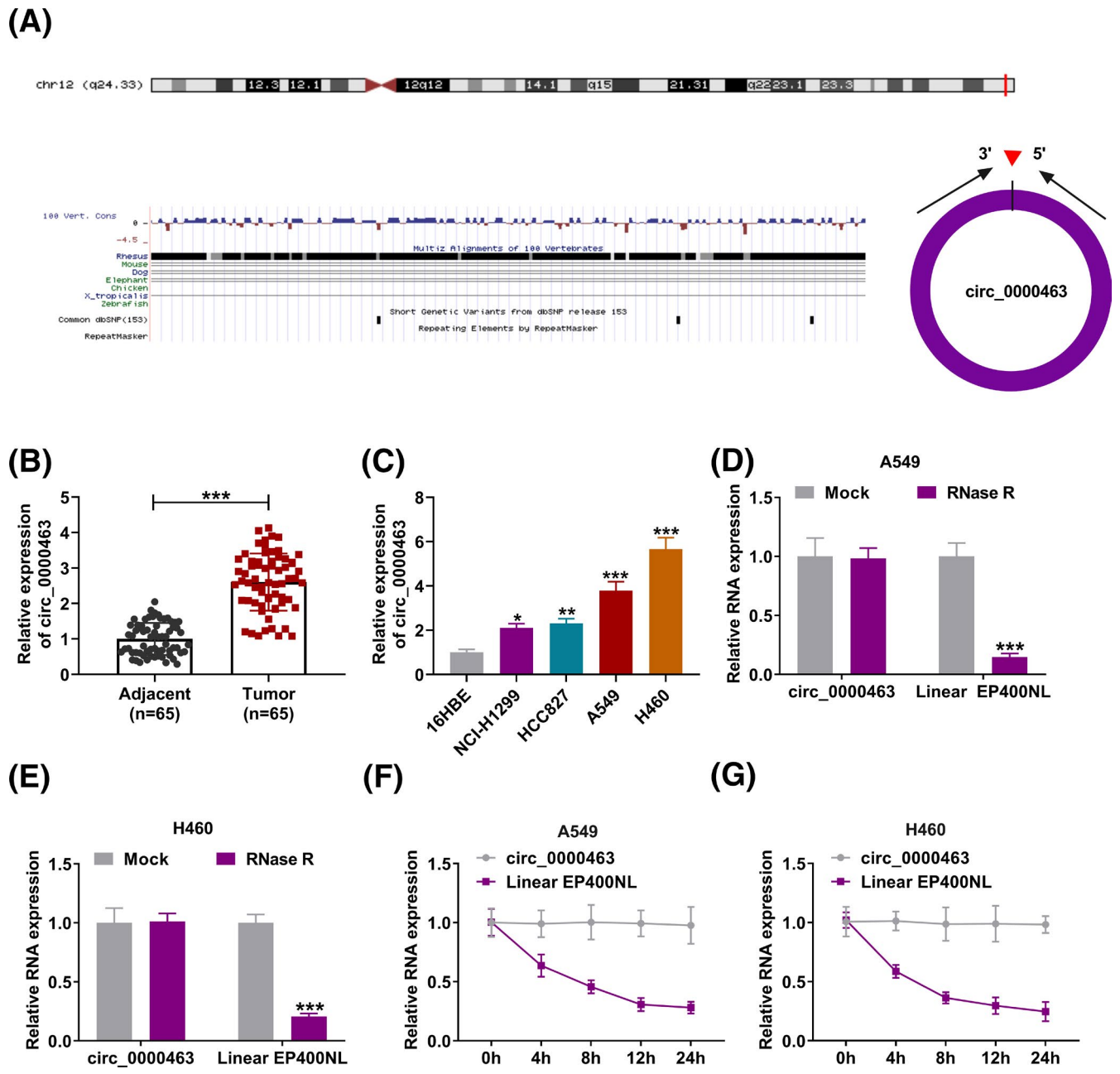

FIGURE 1 Circ_0000463 expression is significantly upregulated in NSCLC tissues and cell lines. (A) The chromosomal location of circ_0000463 was shown. (B) The expression of circ_0000463 was examined by RT-qPCR in 65 pairs of NSCLC and para-cancerous tissues. (C) The expression of circ_0000463 was determined by RT-qPCR in human bronchial epithelioid cell line 16HBE and a panel of NSCLC cell lines (NCI-H1299, HCC827, A549, and H460). (D and E) RNase R treatment assay was conducted to analyze the stability of circ_0000463. (F and G) The stability of circ_0000463 was assessed by Actinomycin D treatment assay. $^{*}p < 0.05$, $^{**}p < 0.01$, $^{***}p < 0.001$

circ_0000463 in NSCLC cells (Figure 2A). Colony formation assay and EdU assay unveiled that circ_0000463 knockdown markedly reduced the number of colonies and the percentage of EdU^{+} cells (Figure 2B, C), which meant that circ_0000463 silencing suppressed the proliferation of NSCLC cells. Circ_0000463 knockdown notably restrained the migration and invasion abilities of NSCLC cells, verified by the reduced rate of wound closure and the decreased number of invaded cells in sh-circ_0000463 group (Figure 2D, E). Circ_0000463 absence triggered the apoptosis of A549 and H460 cells (Figure 2F). In addition, western blot assay data revealed that circ_0000463 silencing downregulated the level of proliferation-associated PCNA and increased the levels of EMT-associated E-cadherin and pro-apoptotic protein Bax (Figure 2G, H), which further meant that circ_0000463 knockdown suppressed the proliferation and EMT and induced the apoptosis of NSCLC cells. These results demonstrated that circ_0000463 silencing restrained the proliferation, migration, and invasion and induced the apoptosis of NSCLC cells.

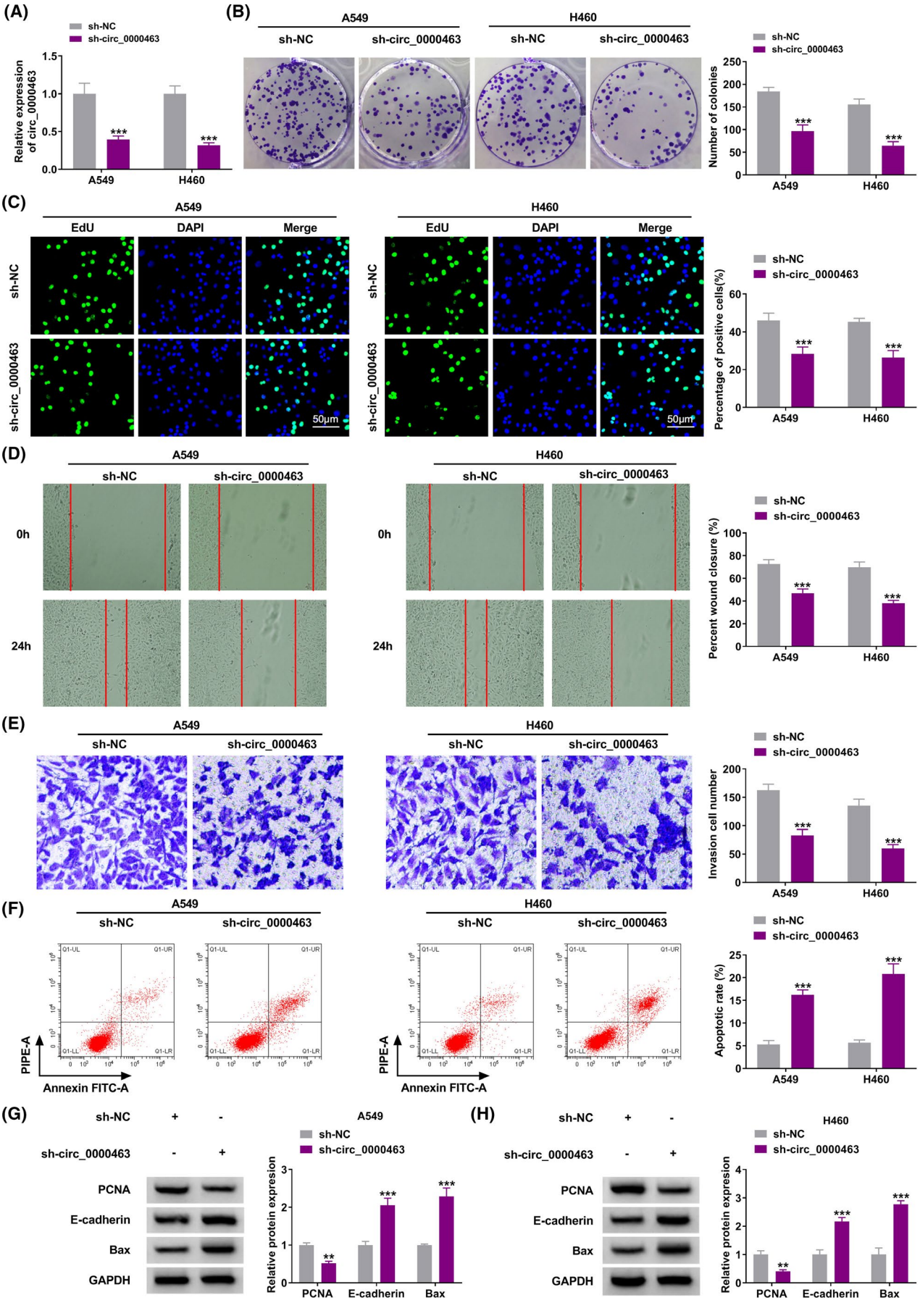
(A)
sh-NC
sh-circ_0000463
Relative expression of circ_0000463
A549
H460
(B)
A549
H460
sh-NC
sh-circ_0000463
Number of colonies
(C)
EdU
DAPI
Merge
50μm
Percentage of positive cells(%)
(D)
0h
24h
Percent wound closure (%)
(E)
Invasion cell number
(F)
PIPE-A
Annexin FITC-A
Apoptotic rate (%)
(G)
PCNA
E-cadherin
Bax
GAPDH
Relative protein expresion
(H)

FIGURE 2 Circ_0000463 absence suppresses the malignant behaviors of NSCLC cells. (A) The expression of circ_0000463 was determined by RT-qPCR in A549 cells and H460 cells stably expressing sh-NC or sh-circ_0000463. (B and C) Colony formation assay and EdU assay were conducted to analyze the effect of circ_0000463 knockdown on the proliferation of NSCLC cells. (D and E) The effects of circ_0000463 silencing on the migration and invasion of NSCLC cells were evaluated by scratch test and transwell invasion assay. (F) Flow cytometry was employed to analyze the impact of circ_0000463 absence on the apoptosis of NSCLC cells. (G and H) Western blot assay was performed to measure the expression of PCNA, E-cadherin, and Bax in circ_0000463-silenced NSCLC cells. $^{**}p < 0.01$, $^{***}p < 0.001$

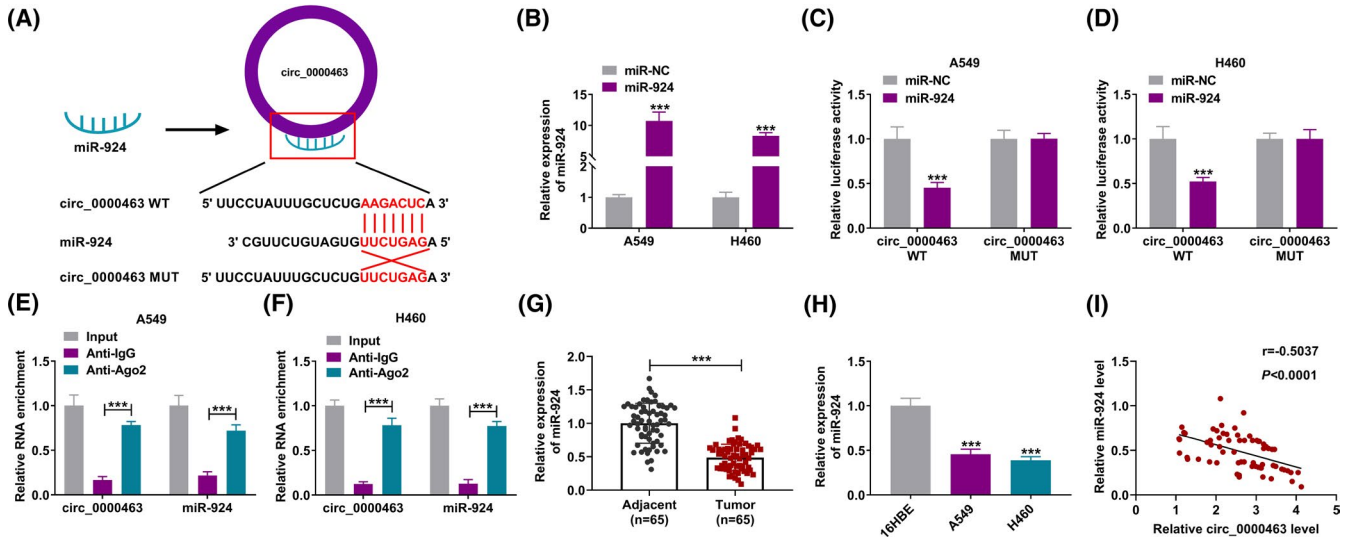

FIGURE 3 Circ_0000463 interacts with miR-924 in NSCLC cells. (A) The supposed binding sites between circ_0000463 and miR-924 were predicted by bioinformatics software circinteractome. (B) The overexpression efficiency of miR-924 was determined by RT-qPCR in A549 and H1299 cells. (C and D) The interaction between circ_0000463 and miR-924 was tested by dual-luciferase reporter assay. (E and F) RIP assay was employed to verify the associated relation between circ_0000463 and miR-924. (G and H) RT-qPCR was conducted to detect the level of miR-924 in 65 pairs of NSCLC and adjacent normal tissues along with 16HBE, A549, and H460 cells. (I) Pearson's correlation analysis was performed to assess the linear correlation between the expression of circ_0000463 and miR-924 in NSCLC tissues. $^{***}p < 0.001$

3.3 | Circ_0000463 interacts with miR-924 in NSCLC cells

We intended to explore the potential mechanism by which circ_0000463 regulated the biological behaviors of NSCLC cells. Circinteractome software (https://circinteractome.irp.nia.nih.gov) revealed the potential binding sequence between circ_0000463 and miR-924 (Figure 3A). The overexpression efficiency of synthesized miR-924 mimics was significant in NSCLC cells (Figure 3B). Subsequently, the target relationship between circ_0000463 and miR-924 was tested by dual-luciferase reporter assay and RIP assay. The luciferase activity of wild-type plasmid (circ_0000463 WT) was markedly reduced by the transfection of miR-924 rather than miR-NC, while the luciferase activity of mutant plasmid (circ_0000463 MUT) remained unchanged by the transfection of miR-924 or miR-NC (Figure 3C, D), which meant that circ_0000463 directly interacted with miR-924 via the predicted sites. Both circ_0000463 and miR-924 were enriched in Ago2 antibody group (Figure 3E, F), suggesting that there was spatial interaction between circ_0000463 and miR-924 in RNA-induced silencing complex (RISC). Circ_0000463 expression was markedly reduced in NSCLC tissues and cell lines (A549 and H460) than that in adjacent normal tissues and 16HBE cell line (Figure 3G, H). Pearson's correlation analysis revealed that miR-924 expression was negatively correlated with circ_0000463 level in NSCLC tissues (Figure 3I). These results suggested that circ_0000463 acted as a molecular sponge for miR-924 in NSCLC cells.

3.4 | Circ_0000463 silencing-mediated anti-tumor effects are largely overturned by the silence of miR-924

RT-qPCR assay showed that the transfection efficiency of in-miR-924 was significant in NSCLC cells (Figure 4A). Considering the target relationship between circ_0000463 and miR-924, we intended to investigate whether circ_0000463 regulated the biological behaviors of NSCLC cells by targeting miR-924, and rescue experiments were conducted. Circ_0000463 knockdown increased the expression of miR-924, and miR-924 expression was decreased again by the introduction of in-miR-924 (Figure 4B). Colony formation assay and EdU assay together demonstrated that circ_0000463 interference-mediated inhibitory effect on the proliferation of NSCLC cells was largely reversed by the silence

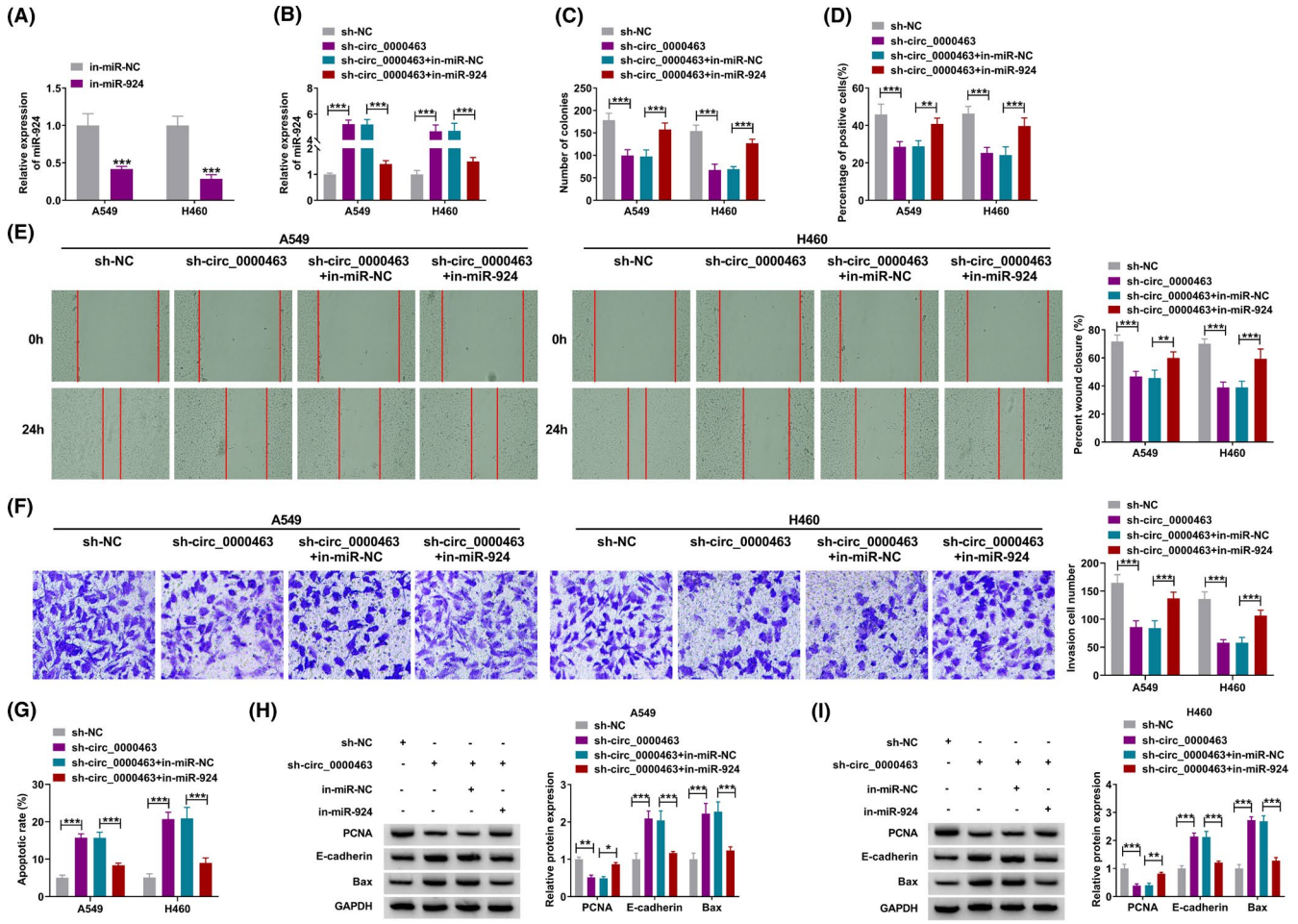

FIGURE 4 Circ_0000463 silencing-mediated anti-tumor effects are largely overturned by the silence of miR-924. (A) The effect of in-miR-924 on the level of miR-924 was analyzed by RT-qPCR in A549 and H460 cells. (B-I) NSCLC cells stably expressing sh-circ_0000463 were transfected with in-miR-924 or in-miR-NC. (B) RT-qPCR was employed to measure the expression of miR-924 in A549 and H460 cells. (C and D) Cell proliferation ability was analyzed by colony formation assay and EdU assay. (E and F) The migration and invasion abilities of NSCLC cells were assessed by scratch test and transwell invasion assay. (G) The apoptotic rate of transfected A549 and H460 cells was analyzed by flow cytometry. (H and I) The protein levels of PCNA, E-cadherin, and Bax in transfected NSCLC cells were determined by western blot assay. $^{*}p < 0.05$, $^{**}p < 0.01$, $^{***}p < 0.001$

of miR-924 (Figure 4C, D). Scratch test and transwell invasion assay together suggested that circ_0000463 absence-mediated suppressive effects on the migration and invasion of NSCLC cells were largely reversed by the knockdown of miR-924 (Figure 4E, F). Circ_0000463 knockdown-induced apoptosis of NSCLC cells was also largely counteracted by the addition of in-miR-924 (Figure 4G). Circ_0000463 knockdown-induced downregulation of PCNA and upregulation of E-cadherin and Bax were largely reversed by the introduction of in-miR-924 (Figure 4H, I). These findings indicated that circ_0000463 silencing suppressed the biological behaviors of NSCLC cells largely by upregulating miR-924.

3.5 | miR-924 interacts with SLC1A5 in NSCLC cells

The working mechanism of miR-924 in NSCLC cells was then explored. Targetscan bioinformatics software (http://www.targetscan.org) predicted that the 3'UTR of SLC1A5 possessed the complementary sites with miR-924 (Figure 5A). Dual-luciferase reporter assay was conducted to verify the interaction between miR-924 and SLC1A5. The luciferase activity of wild-type plasmid (SLC1A5 3'UTR WT) was dramatically reduced by the transfection of miR-924 but not that of miR-NC, and the luciferase activity of mutant plasmid (SLC1A5 3'UTR MUT) was similar by the transfection of miR-924 or miR-NC (Figure 5B, C), suggesting that miR-924 interacted with the 3'UTR of SLC1A5 via the putative sites. RT-qPCR and western blot assay showed that SLC1A5 mRNA and protein expression was up-regulated in NSCLC tissues compared with adjacent normal tissues (Figure 5D, 5E). In addition, IHC assay data further confirmed the high expression of SLC1A5 in NSCLC tissues in comparison with that in adjacent normal tissues (Figure 5F). The protein level of SLC1A5 was increased in A549 and H460 cell lines compared with 16HBE cell line (Figure 5G). Pearson's correlation analysis showed that SLC1A5 mRNA level was negatively correlated with miR-924

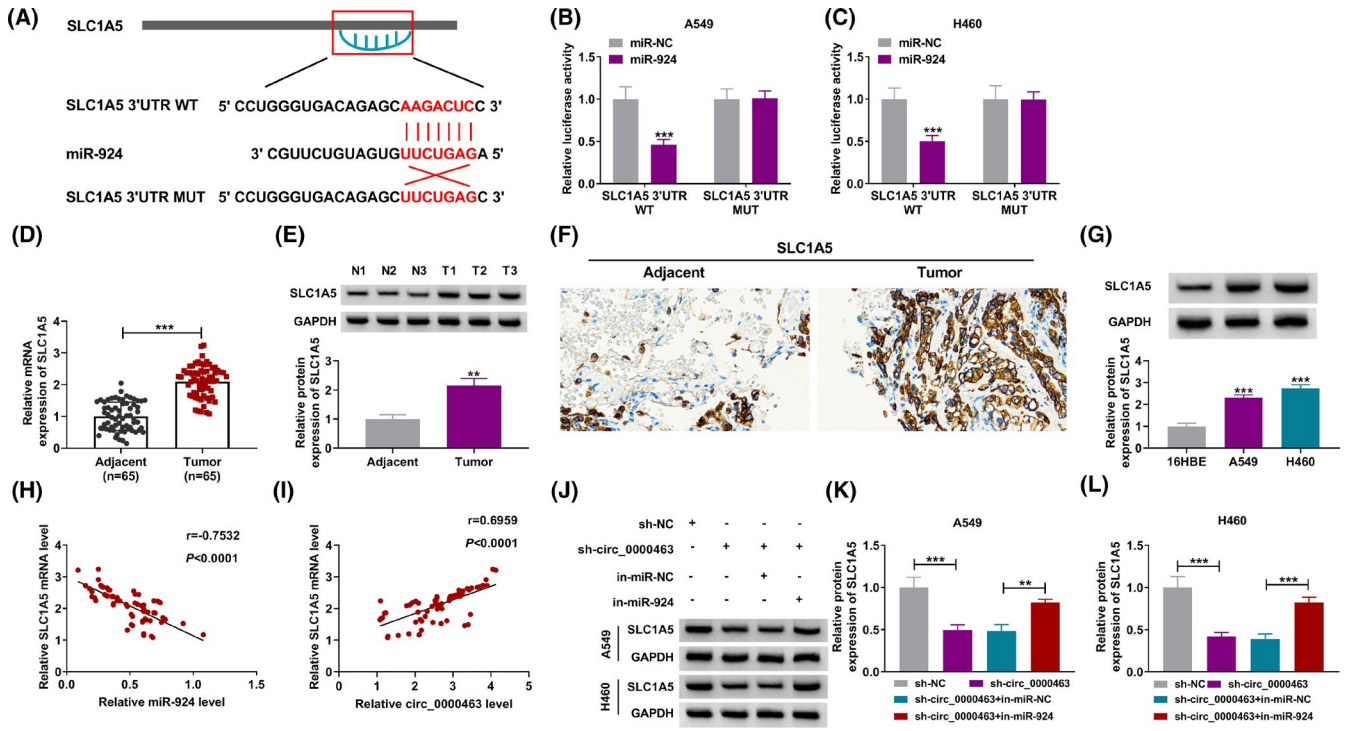

FIGURE 5 miR-924 interacts with SLC1A5 in NSCLC cells. (A) Bioinformatics software targetscan was used to predict the targets of miR-924, and SLC1A5 was predicted as one of the candidate targets of miR-924. (B and C) Dual-luciferase reporter assay was employed to verify the associated relation between miR-924 and SLC1A5. (D and E) The mRNA and protein expression of SLC1A5 was determined in NSCLC and para-cancerous tissues by RT-qPCR and western blot assay, respectively. (F) The protein level of SLC1A5 was examined in NSCLC and adjacent normal tissues by IHC assay. (G) The protein level of SLC1A5 was detected in 16HBE, A549, and H460 cells by western blot assay. (H and I) Pearson's correlation analysis was carried out to assess the linear correlation between the expression of SLC1A5 mRNA and miR-924 or circ_0000463. (J-L) The effect of circ_0000463 silencing alone or together with miR-924 absence on the protein expression of SLC1A5 was analyzed by western blot assay. $^{**}p < 0.01$, $^{***}p < 0.001$

expression, and was positively correlated with circ_0000463 expression in NSCLC tissues (Figure 5H, I). Circ_0000463 silencing reduced SLC1A5 protein expression, and SLC1A5 protein level was restored by the addition of in-miR-924 (Figure 5J–5L). Taken together, SLC1A5 was a direct target of miR-924, and circ_0000463 can positively regulate SLC1A5 expression by sponging miR-924 in NSCLC cells.

3.6 | SLC1A5 overexpression largely reverses miR-924 overexpression-mediated anti-tumor effects in NSCLC cells

Western blot assay showed that the transfection efficiency of SLC1A5 plasmid was significant in NSCLC cells (Figure 6A). To explore whether miR-924 regulated the biological behaviors of NSCLC cells by targeting SLC1A5, rescue experiments were performed. miR-924 overexpression reduced the expression of SLC1A5 protein level, and the protein level of SLC1A5 was largely rescued by the introduction of SLC1A5 plasmid (Figure 6B). miR-924 overexpression reduced the number of colonies and the percentage of EdU^+ cells (Figure 6C, D), which meant that miR-924 overexpression suppressed the proliferation of NSCLC cells. Moreover, the introduction of SLC1A5 plasmid largely recovered the proliferation ability of NSCLC cells (Figure 6C, D). The migration and invasion abilities of NSCLC cells were suppressed by the overexpression of miR-924, which were largely recovered by the introduction of SLC1A5 plasmid (Figure 6E, F). miR-924 overexpression induced the apoptosis of NSCLC cells, which was alleviated by the addition of SLC1A5 plasmid (Figure 6G). miR-924 accumulation reduced PCNA level and increased the expression of E-cadherin and Bax, and these effects were alleviated by the introduction of SLC1A5 plasmid (Figure 6H, I). Taken together, miR-924 overexpression suppressed the biological behaviors of NSCLC cells largely by down-regulating SLC1A5.

3.7 | Circ_0000463 silencing suppresses the glutamine metabolism of NSCLC cells by targeting miR-924/SLC1A5 axis

Abnormal energy metabolism is an important hallmark of cancer.[19] Considering that SLC1A5 plays a pivotal regulatory role in the transportation of glutamine,[13] we then analyzed the effect of

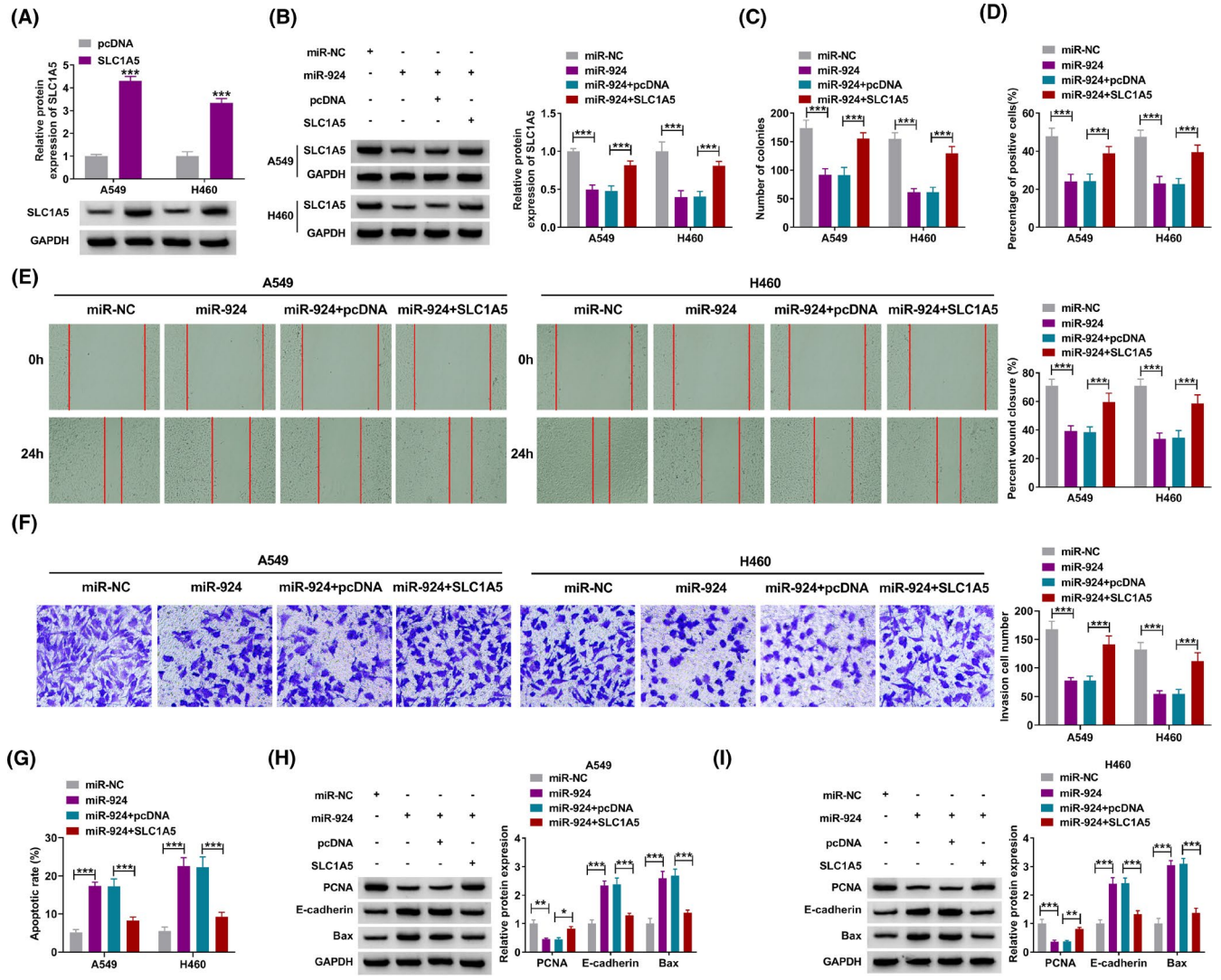

FIGURE 6 SLC1A5 overexpression largely reverses miR-924 overexpression-mediated anti-tumor effects in NSCLC cells. (A) Western blot assay was conducted to confirm the effect of SLC1A5 plasmid on the expression of SLC1A5 in A549 and H460 cells. (B-I) A549 and H460 cells were transfected with miR-NC, miR-924, miR-924 + pcDNA, or miR-924 + SLC1A5. (B) The protein level of SLC1A5 was examined in transfected NSCLC cells by western blot assay. (C and D) Colony formation assay and EdU assay were carried out to assess the proliferation ability of NSCLC cells. (E and F) Scratch test and transwell invasion assay were implemented to analyze cell migration and invasion abilities. (G) The apoptotic rate of NSCLC cells was assessed by flow cytometry. (H and I) The protein levels of PCNA, E-cadherin, and Bax were detected by western blot assay. $^{*}p < 0.05$, $^{**}p < 0.01$, $^{***}p < 0.001$

circ_0000463/miR-924/SLC1A5 axis on the glutamine metabolism of NSCLC cells. Circ_0000463 absence restrained the uptake of glutamine and the production of glutamate and α-ketoglutarate, which were all largely diminished by the addition of in-miR-924 (Figure 7A–C), suggesting that circ_0000463 knockdown suppressed the glutamine metabolism of NSCLC cells largely by upregulating miR-924. Moreover, we found that miR-924 overexpression inhibited the glutamine metabolism of NSCLC cells, and this suppressive effect was attenuated by the addition of SLC1A5 plasmid (Figure 7D–F), indicating that miR-924 suppressed the glutamine metabolism of NSCLC cells largely by downregulating SLC1A5. These results demonstrated that circ_0000463 contributed to the glutamine metabolism of NSCLC cells through mediating miR-924/SLC1A5 axis.

3.8 | Circ_0000463 absence suppresses xenograft tumor growth in vivo

The effects of circ_0000463 knockdown on the formation and growth of xenograft tumors were explored via mice xenograft model. The volume and weight were smaller or lighter in xenograft tumors derived from A549 cells stably expressing sh-circ_0000463 compared with sh-NC group (Figure 8A–C), suggesting the suppressive effect of circ_0000463 absence on tumor growth. The expression of circ_0000463 and SLC1A5 protein was reduced in tumor tissues in sh-circ_0000463 group compared with sh-NC group (Figure 8D, F). We also found that miR-924 level was markedly upregulated in sh-circ_0000463 group compared with sh-NC group (Figure 8E). These results showed that circ_0000463 knockdown suppressed

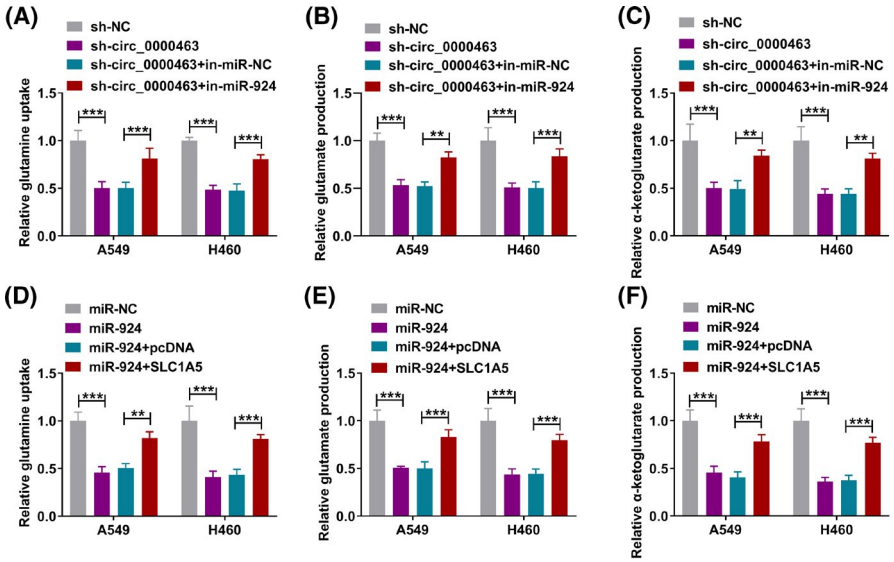

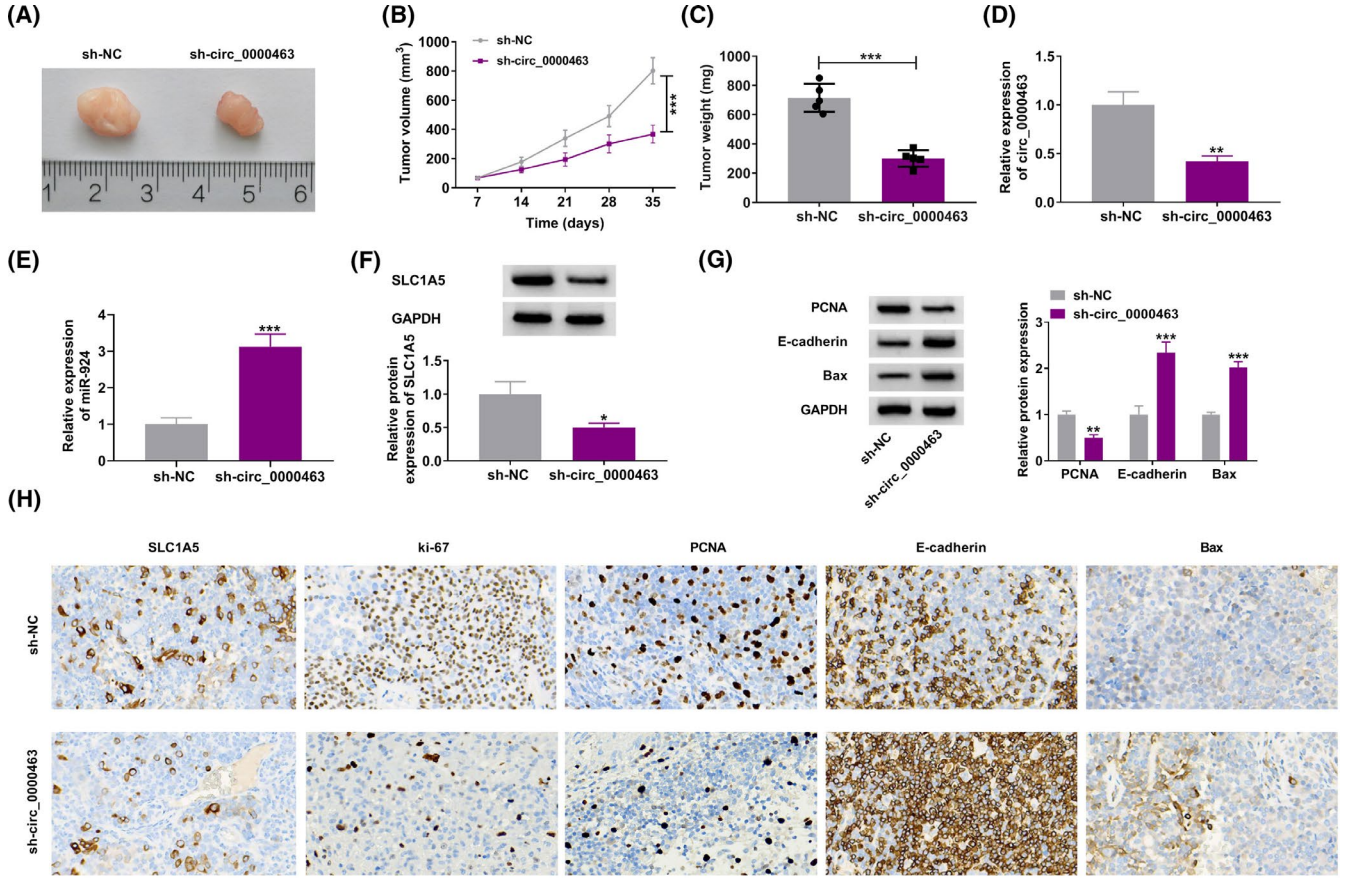

FIGURE 7 Circ_0000463 silencing suppresses the glutamine metabolism of NSCLC cells by targeting miR-924/SLC1A5 axis. (A-C) The effect of circ_0000463 knockdown alone or together with miR-924 silencing on the uptake of glutamine and the production of glutamate and α-ketoglutarate was analyzed using their corresponding kits. (D-F) The consumption of glutamine and the production of glutamate and α-ketoglutarate in A549 and H460 cells transfected with miR-924 alone or together with SLC1A5 plasmid were assessed using their matched kits. $^{**}p < 0.01$, $^{***}p < 0.001$

FIGURE 8 Circ_0000463 absence suppresses xenograft tumor growth *in vivo*. (A-C) The effects of circ_0000463 silencing on the volume and weight of xenograft tumors were explored. (D and E) RT-qPCR was conducted to measure the expression of circ_0000463 and miR-924 in xenograft tumor tissues derived from A549 cells stably expressing sh-NC or sh-circ_0000463. (F and G) The impacts of circ_0000463 knockdown on the protein levels of SLC1A5, PCNA, E-cadherin, and Bax in tumor tissues were assessed by western blot assay. (H) IHC assay was carried out to determine the protein levels of SLC1A5, ki-67, PCNA, E-cadherin, and Bax in tumor tissues in sh-NC and sh-circ_0000463 groups. $^{*}p < 0.05$, $^{**}p < 0.01$, $^{***}p < 0.001$

xenograft tumor growth at least partly by targeting miR-924/SLC1A5 axis. Circ_0000463 silencing reduced PCNA expression and increased the levels of E-cadherin and Bax in tumor tissues (Figure 8G). IHC assay data unveiled that the expression of SLC1A5, ki-67, and PCNA was reduced in sh-circ_0000463 group, whereas the levels of E-cadherin and Bax were upregulated in sh-circ_0000463 group (Figure 8H). These results demonstrated that circ_0000463 knockdown repressed xenograft tumor growth in vivo.

4 | DISCUSSION

CircRNAs are a class of conserved circular RNA molecules, which can be divided into noncoding circRNAs and coding circRNAs.[9,20–23] Accumulating evidence have shown that circRNAs regulate multiple biological behaviors of tumor cells, such as cell proliferation, apoptosis, and motility.[24] Zhong et al.[25] found that circ_0005075 facilitates the growth and invasion abilities of colorectal cancer cells. Sun et al.[6] demonstrated that circ_0000376 facilitates the growth, motility, and chemo-resistance of NSCLC cells. A previous study reported that the level of circ_0000463 is abnormally elevated in lung cancer.[7] However, the function of circ_0000463 in NSCLC progression remains largely unknown. Through analyzing the expression pattern of circ_0000463, we found that circ_0000463 expression was notably elevated in NSCLC tissues and cell lines, which was consistent with former article.[7] RNase R and actinomycin D treatment experiments together demonstrated that circ_0000463 was indeed a circular transcript. Then, knockdown experiments were conducted to explore the biological function of circ_0000463 in NSCLC cells. Circ_0000463 absence restrained the proliferation, migration, and invasion abilities and elevated the apoptotic rate of NSCLC cells, suggesting that circ_0000463 absence suppressed NSCLC progression in vitro. These results indicated the potential of circ_0000463 to be a novel therapeutic target for NSCLC. Nevertheless, further experiments are needed to explore this issue.

CircRNAs are implicated in the modulation of cell functions by acting as miRNA sponges in a competing endogenous RNA (ceRNA) manner.[26] To investigate the working mechanism of circ_0000463, we predicted the potential miRNA targets of circ_0000463. We confirmed the associated relation between circ_0000463 and miR-924. Previous studies reported that miR-924 suppressed the progression of hepatocellular carcinoma[11] and NSCLC.[12] Consistently, we found that miR-924 overexpression inhibited the biological properties of NSCLC cells. Furthermore, circ_0000463 knockdown-induced inhibitory effects on the malignant properties of NSCLC cells were largely reversed by the knockdown of miR-924, indicating that circ_0000463 absence restrained NSCLC progression largely by upregulating the anti-tumor molecule miR-924.

SLC1A5 is implicated in the modulation of cancer development.[27] Zhuang et al. found that SLC1A5 contributed to the proliferation capacity and motility of papillary thyroid cancer cells.[16] Xue et al.[18] demonstrated that SLC1A5 facilitated the proliferation and motility and decreased the apoptotic rate of NSCLC cells. Here, SLC1A5 was identified as a molecular target of miR-924 in NSCLC cells. SLC1A5 abundance was aberrantly elevated in NSCLC tissue specimens and cell lines. Moreover, SLC1A5 was reversely modulated by miR-924 in NSCLC cells. To investigate whether miR-924 played an anti-tumor activity by negatively regulating SLC1A5, we cotransfecting NSCLC cells with miR-924 and SLC1A5 to perform rescue experiments. The suppressive effects in NSCLC progression induced by miR-924 overexpression were largely overturned by the accumulation of SLC1A5, suggesting that miR-924 overexpression suppressed NSCLC progression largely by downregulating SLC1A5 in vitro. We also found that circ_0000463 absence reduced SLC1A5 protein expression partly by up-regulating miR-924 in NSCLC cells, suggesting that circ_0000463 positively regulated SLC1A5 expression by sequestering miR-924 in NSCLC cells.

SLC1A5 is a pivotal transporter for the consumption of glutamine,[17] which has been identified to be an important molecule for the growth of cancer cells.[28,29] Then, we analyzed whether circ_0000463/miR-924/SLC1A5 axis was involved in the glutamine metabolism of NSCLC cells. The results indicated that circ_0000463 absence suppressed glutamine uptake and the production of glutamate and α-ketoglutarate by targeting miR-924/SLC1A5 signaling, demonstrating that circ_0000463 knockdown restrained the glutamine metabolism of NSCLC cells through mediating miR-924/SLC1A5 signaling.

Considering the pro-tumor role of circ_0000463 in regulating the biological behaviors of NSCLC cells in vitro, we subsequently analyzed whether it exerted a similar role in regulating the growth of xenograft tumors in vivo. The data revealed that circ_0000463 knockdown suppressed xenograft tumors growth at least partly by regulating miR-924/SLC1A5 axis in vivo.

However, there were several limitations in our study that should be noted. There were no data about the association between the expression of circ_0000463/miR-924/SLC1A5 axis and the clinicopathologic features of NSCLC patients. Moreover, the circRNAs/miRNAs/mRNAs axes are cross-talked with each other, and this study only focused on the linear circ_0000463/miR-924/SLC1A5 axis in NSCLC. Therefore, the results may be unpersuasive to some extent. In the future, more experiments are needed to confirm the findings in this study.

In conclusion, our study proved that circ_0000463 interference hindered the proliferation, migration, invasion, and glutamine metabolism and elevated the apoptotic rate of NSCLC cells by targeting miR-924/SLC1A5 signaling, which gave new insights into the molecular mechanism of NSCLC pathogenesis.

CONFLICT OF INTEREST

The authors declare that they have no competing interests.

DATA AVAILABILITY STATEMENT

The datasets used and analyzed during the current study are available from the corresponding author on reasonable request.

ORCID

Ying Zhao https://orcid.org/0000-0001-7776-5114

REFERENCES

1. Torre LA, Siegel RL, Jemal A. Lung cancer statistics. *Adv Exp Med Biol*. 2016;893:1-19.
2. Friedlaender A, Addeo A, Russo A, Gregorc V, Cortinovis D, Rolfo CD. Targeted therapies in early stage NSCLC: hype or hope? *Int J Mol Sci*. 2020;21:6329.

3. Duma N, Santana-Davila R, Molina JR. Non-small cell lung cancer: epidemiology, screening, diagnosis, and treatment. *Mayo Clin Proc*. 2019;94:1623-1640.
4. Zhang Z, Yang T, Xiao J. Circular RNAs: promising biomarkers for human diseases. *EBioMedicine*. 2018;34:267-274.
5. Xu P, Wang L, Xie X, et al. Hsa_circ_0001869 promotes NSCLC progression via sponging miR-638 and enhancing FOSL2 expression. *Aging (Albany NY)*. 2020;12:23836-23848.
6. Sun H, Chen Y, Fang YY, et al. Circ_0000376 enhances the proliferation, metastasis, and chemoresistance of NSCLC cells via repressing miR-384. *Cancer Biomark*. 2020;29:463-473.
7. Liu ZH, Yang SZ, Chen XT, et al. Correlations of hsa_circ_0046264 expression with onset, pathological stage and chemotherapy resistance of lung cancer. *Eur Rev Med Pharmacol Sci*. 2020;24:9511-9521.
8. Hansen TB, Jensen TI, Clausen BH, et al. Natural RNA circles function as efficient microRNA sponges. *Nature*. 2013;495:384-388.
9. Kristensen LS, Andersen MS, Stagsted LVW, Ebbesen KK, Hansen TB, Kjems J. The biogenesis, biology and characterization of circular RNAs. *Nat Rev Genet*. 2019;20:675-691.
10. Panda AC. Circular RNAs act as miRNA sponges. *Adv Exp Med Biol*. 2018;1087:67-79.
11. Fan H, Lv P, Mu T, et al. LncRNA n335586/miR-924/CKMT1A axis contributes to cell migration and invasion in hepatocellular carcinoma cells. *Cancer Lett*. 2018;429:89-99.
12. Wang H, Chen X, Yang B, Xia Z, Chen Q. MiR-924 as a tumor suppressor inhibits non-small cell lung cancer by inhibiting RHBDD1/Wnt/β-catenin signaling pathway. *Cancer Cell Int*. 2020;20:491.
13. van Geldermalsen M, Wang Q, Nagarajah R, et al. ASCT2/SLC1A5 controls glutamine uptake and tumour growth in triple-negative basal-like breast cancer. *Oncogene*. 2016;35:3201-3208.
14. Ding J, Gou Q, Jin J, Shi J, Liu Q, Hou Y. Metformin inhibits PPARδ agonist-mediated tumor growth by reducing Glut1 and SLC1A5 expressions of cancer cells. *Eur J Pharmacol*. 2019;857:172425.
15. Osman I, He X, Liu J, et al. TEAD1 (TEA Domain Transcription Factor 1) promotes smooth muscle cell proliferation through upregulating SLC1A5 (Solute Carrier Family 1 Member 5)-mediated glutamine uptake. *Circ Res*. 2019;124:1309-1322.
16. Zhuang X, Tong H, Ding Y, et al. Long noncoding RNA ABHD11-AS1 functions as a competing endogenous RNA to regulate papillary thyroid cancer progression by miR-199a-5p/SLC1A5 axis. *Cell Death Dis*. 2019;10:620.
17. Hassanein M, Hoeksema MD, Shiota M, et al. SLC1A5 mediates glutamine transport required for lung cancer cell growth and survival. *Clin Cancer Res*. 2013;19:560-570.
18. Xue M, Hong W, Jiang J, Zhao F, Gao X. Circular RNA circ-LDLRAD3 serves as an oncogene to promote non-small cell lung cancer progression by upregulating SLC1A5 through sponging miR-137. *RNA Biol*. 2020;17:1811-1822.
19. Hanahan D, Weinberg RA. Hallmarks of cancer: the next generation. *Cell*. 2011;144:646-674.
20. Wu P, Mo Y, Peng M, et al. Emerging role of tumor-related functional peptides encoded by lncRNA and circRNA. *Mol Cancer*. 2020;19:22.
21. Lu Y, Li Z, Lin C, Zhang J, Shen Z. Translation role of circRNAs in cancers. *J Clin Lab Anal*. 2021;35:e23866.
22. Li Z, Ruan Y, Zhang H, Shen Y, Li T, Xiao B. Tumor-suppressive circular RNAs: Mechanisms underlying their suppression of tumor occurrence and use as therapeutic targets. *Cancer Sci*. 2019;110:3630-3638.
23. Zhao W, Zhang Y, Zhu Y. Circular RNA circβ-catenin aggravates the malignant phenotype of non-small-cell lung cancer via encoding a peptide. *J Clin Lab Anal*. 2021;35:e23900.
24. Kristensen LS, Hansen TB, Venø MT, Kjems J. Circular RNAs in cancer: opportunities and challenges in the field. *Oncogene*. 2018;37:555-565.
25. Zhong D, Li P, Gong PY. Hsa_circ_0005075 promotes the proliferation and invasion of colorectal cancer cells. *Int J Biol Markers*. 2019;34:284-291.
26. Qi X, Zhang DH, Wu N, Xiao JH, Wang X, Ma W. ceRNA in cancer: possible functions and clinical implications. *J Med Genet*. 2015;52:710-718.
27. Scalise M, Pochini L, Console L, Losso MA, Indiveri C. The human SLC1A5 (ASCT2) amino acid transporter: from function to structure and role in cell biology. *Front Cell Dev Biol*. 2018;6:96.
28. Gkiouli M, Biechl P, Eisenreich W, Otto AM. Diverse roads taken by (13)C-glucose-derived metabolites in breast cancer cells exposed to limiting glucose and glutamine conditions. *Cells*. 2019;8:1113.
29. Kappler M, Pabst U, Weinholdt C, et al. Causes and consequences of A glutamine induced normoxic HIF1 activity for the tumor metabolism. *Int J Mol Sci*. 2019;20:4742.

How to cite this article: Liu Y, Wang S, Pan S, Yan Q, Li Y, Zhao Y. Circ_0000463 contributes to the progression and glutamine metabolism of non-small-cell lung cancer by targeting miR-924/SLC1A5 signaling. *J Clin Lab Anal*. 2022;36:e24116. doi:10.1002/jcla.24116